

SIMULATION FOR LCLS-II HARD X-RAY SELF-SEEDING SCHEME*

C. Yang^{1,2†}, J. Wu^{1‡}, Y. Feng¹, Y. Hong³, J. Krzywinski¹, T. O. Raubenheimer¹
C.-Y. Tsai¹, X. Wang^{1,4}, B. Yang³, M. Yoon^{1,5}, G. Zhou^{1,6}, H. Deng⁴, D. He²

¹SLAC National Accelerator Laboratory, Menlo Park, California, USA

²NSRL, University of Science and Technology of China, Hefei, Anhui, China

³University of Texas at Arlington, Arlington, Texas, USA

⁴Shanghai Institute of Applied Physics, Chinese Academy of Sciences, Shanghai, China

⁵Department of Physics, Pohang University of Science and Technology, Pohang, Korea

⁶Institute of High Energy Physics, and UCAS, Chinese Academy of Sciences, Beijing, China

Abstract

Typical SASE FELs have poor temporal coherence because of starting from shot noise. Self-seeding scheme is an approach to improve the longitudinal coherence. The single crystal monochromator self-seeding has been in successful operation in LCLS. For the high repetition rate LCLS-II machine, for damage consideration, it was initially proposed to have a two-stage self-seeding scheme, yet we have found the two-stage self-seeding scheme has no advantage over one-stage self-seeding scheme. In this paper, we investigate the optimal self-seeding configuration of LCLS-II for different photon energies, and present a comparison between one-stage and two-stage self-seeding scheme of LCLS-II.

INTRODUCTION

The first hard X-ray FEL (the Linac Coherent Light Source, LCLS) at SLAC, has served as an important tool for the research in materials, chemistry, and biology. The LCLS has been successfully operated both in Self-Amplified Spontaneous Emission (SASE) mode [1] and self-seeding mode [2]. Conventional SASE FEL has fully transverse coherence, but has limited temporal coherence because of starting from shot noise. Self-seeding scheme is proposed to generate fully coherent FEL both in transverse and temporal dimensions [3]. A grating monochromator is used in soft X-ray regime [3], while a single crystal monochromator is adopted in the hard X-ray regime [4].

Self-seeding FELs consist of two undulators separated by a monochromator and a by-pass chicane. After the first undulator, the radiation goes through the monochromator, which can filter the SASE X-ray pulse to a desired narrow bandwidth. In parallel, the electron beam passes through the chicane, which can wash out the micro-bunching and compensate the optical path delay caused by the monochromator. The monochromatic seed and the electron bunch are recombined at the entrance of the second undulator, through which the radiation is amplified up to saturation.

For high repetition rate FEL facilities, the heat load, vibration and shock wave of the crystal monochromator may

degrade the seed quality. Therefore, the damage threshold of the crystal is very important. If diamond is heated instantaneously above its graphitization temperature of 1400 K, corresponding to an atomic dose of 0.213 eV/atom [5], the process of graphitization could commence. If the instantaneous dose is lower than the graphitization threshold but the diamond crystal is impinged by high repetition rate X-ray pulses, the thermal damage may happen. For 8 keV case, the measured damage threshold is 8 kW/mm² [6]. Two-stage self-seeding is proposed to share the heat load on the crystal and purify the output spectrum [7].

In practice, when we do the self-seeding configuration optimization, we need to obey the following three rules no matter it is one-stage or two-stage scheme. The first is that the location of the crystal should be within the exponential gain region, so that energy loss and energy spread induced by the FEL process are small enough to allow for lasing in the output undulator. Secondly, the heat load should be smaller than the damage threshold. Thirdly, the seed power should be enough to dominate over the shot noise power.

LCLS-II project is designed to operate at repetition rate of 1MHz. The lower photon energy limit of LCLS-II self-seeding scheme is 3.25 keV, and the upper limit is 4.25 keV. In our previous LCLS-II hard X-ray self-seeding (HXRSS) simulation work, we pointed out that the two-stage scheme has no advantage over the one-stage scheme [8]. In this paper, we will focus on the optimization of the one-stage self-seeding configuration which works for all of the photon energy range, and make a comparison between the one-stage and two-stage self-seeding schemes.

NUMERICAL SIMULATION

Undulator Baseline

The current hard X-ray undulator baseline of LCLS-II has 34 slots. 32 slots are used to install undulators and 2 slots are used to install the self-seeding stations of which the locations are slot 8 and slot 16 shown in Fig. 1 corresponding to Line 1. For the one-stage self-seeding scheme, neither the slot 8 nor slot 16 is the optimal self-seeding station. According to the optimization, we suggest to move the second self-seeding station from slot 16 to slot 14 shown in Fig. 1 corresponding to Line 2.

* The work was supported by the US Department of Energy (DOE) under contract DE-AC02-76SF00515 and the US DOE office of Science Early Career Research Program grant FWP-2013-SLAC-100164.

† chuany@slac.stanford.edu; yc199025@mail.ustc.edu.cn

‡ jhwu@slac.stanford.edu

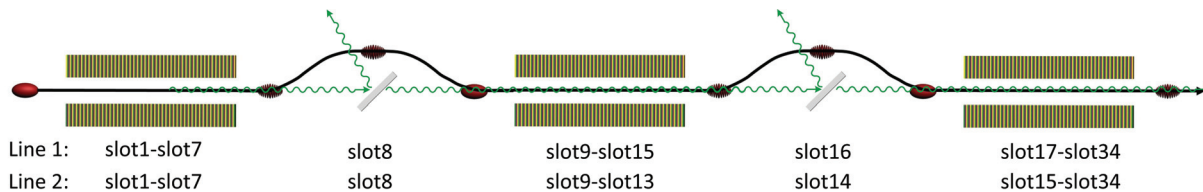


Figure 1: (Line 1) The current undulator baseline of LCLS-II. The slot 8 and slot 16 are reserved for self-seeding station. (Line 2) The optimal one-stage undulator baseline. The self-seeding station is at slot 14.

Electron Beam and Crystal Parameters

In this part, we will present the self-seeding configuration study with the help of FEL code GENESIS [9]. We will report the facility study based on 20 FEL runs. For the photon energies from 3.25 keV to 4.25 keV, we use symmetric diamond (111) as the monochromator, and the crystal thickness is 30 μm . The transmissivity of the crystal is calculate with the help of Xop2.4 [10], and the phase of the transmissivity is retrieved by Kramers–Kronig relations. The overall electron beam parameters in our simulation is shown in Table 1.

Table 1: Relevant Simulation Parameters in This Paper

Parameters		Units
Beam energy	4.0	GeV
Energy spread	0.6	MeV
Peak current	800	A
Normalized emittance	0.35	$\mu\text{m rad}$
Undulator period	2.6	cm
Photon energy	3.25-4.25	keV
Charge	100	pC

The start-to-end electron beam phase space and the emittance as a function of bunch length are shown in Fig. 2. The normalized emittance of the core is about 0.35 $\mu\text{m rad}$, and the current around the core is about 800 A. The energy loss of the electron beam caused by the wake field inside the undulators is also accounted in Fig. 2.

The SASE gain curves for different photon energies are shown in Fig.3. In low photon energy range, the SASE gain process around the slot 16 is close to saturation. That means the slot 16 is not the optimal crystal location for one-stage self-seeding scheme. According to the FEL simulations for different photon energies, we pick up the slot 14 as the optimal location for one-stage self-seeding scheme.

Lower Limit: 3.25 keV

In the simulation, the average beta-function is 12 m. For one-stage scheme, we turn off 2 undulator cells of the first undulator part. That is, the first undulator part consists of 10 undulator cells. The average power density on the crystal is 260 W/mm^2 which is smaller than the damage threshold, the seed power after the crystal is 450 kW and the output pulse energy is 110 μJ . For two-stage self-seeding scheme, the seed power after the first crystal is about 20 kW which

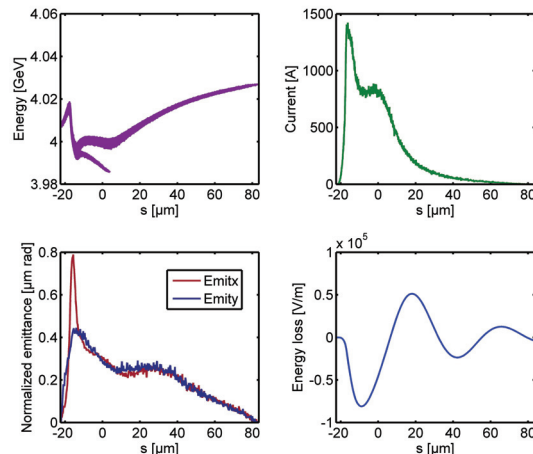


Figure 2: Start to end beam at the entrance of the undulator. (Top left) Electron beam phase space. (Top right) Current distribution. (Bottom left) Normalized emittance as a function of bunch length. (Bottom right) Electron energy loss caused by the undulators wakefields.

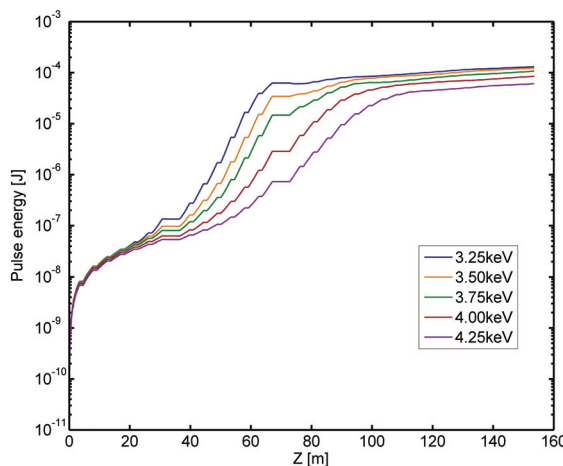


Figure 3: The SASE gain curves of LCLS-II.

is not enough to dominate the shot noise, and the signal to noise ratio (SNR) before the second crystal is about 20. The average power density on the first crystal and the second crystal are 24 W/mm^2 and 430 W/mm^2 respectively, which are also smaller than the damage threshold. The simulation results are summarized in Table 2.

Content from this work may be used under the terms of the CC BY 3.0 licence (© 2018). Any distribution of this work must maintain attribution to the author(s), title of the work, publisher, and DOI.

Table 2: 3.25 keV simulation results. P_s is the average seed power. P_d is the power density on the crystal. $M1$, $M2$ are the diamond monochromators. E_p is the pulse energy. std is the standard deviation.

Parameters	one-stage	two-stage	Units
P_s after M1	-	20	kW
P_s after M2	0.45	1.2	MW
P_d on M1	260±31(<i>std</i>)	24±1(<i>std</i>)	W/mm ²
P_d on M2	-	430±40(<i>std</i>)	W/mm ²
SNR at M2	-	20	-
SNR at Sat.	350	400	-
Output E_p	110	97.4	μJ

The SNR of one-stage and two-stage self-seeding at saturation are 350 and 400 respectively shown in Fig. 4. We still can improve the SNR of one-stage scheme at saturation by using 11 undulator cells at the first undulator part. However, the output pulse energy of one-stage is large than that of two-stage.

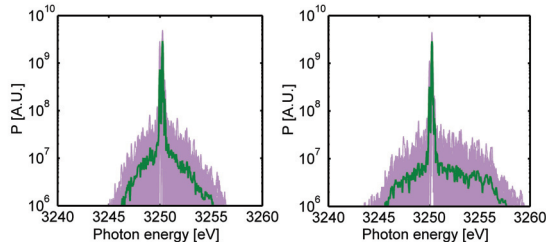


Figure 4: (Left) The saturation spectrum of 3.25 keV one-stage self-seeding. (Right) The saturation spectrum of 3.25 keV two-stage self-seeding. The green curve refers to the average. The purple curves refer to single shot.

Upper Limit: 4.25 keV

In this case, the average beta-function is 14 m. For the one-stage scheme, the first undulator part consists of 12 undulator cells. The average power density on the crystal is 27 W/mm² which is smaller than the damage threshold.

Table 3: 4.25 keV simulation results. P_s is the average seed power. P_d is the power density on the crystal. $M1$, $M2$ is the diamond monochromator. E_p is the pulse energy. std is the standard deviation.

Parameters	one-stage	two-stage	Units
P_s after M1	-	10	kW
P_s after M2	125	500	kW
P_d on M1	27±1.4(<i>std</i>)	6±0.1(<i>std</i>)	W/mm ²
P_d on M2	-	122±16(<i>std</i>)	W/mm ²
SNR at M2	-	15	-
SNR at Sat.	90	80	-
Output E_p	43.13	44.84	μJ

For the two-stage self-seeding scheme, the average power density on the first crystal and the second crystal are 6 W/mm² and 122 W/mm² respectively which are smaller than the damage threshold. The seed power after the first crystal is 10 kW which is even smaller than that of 3.25 keV case, and the SNR before the second crystal is about 15. The simulation results are summarized in Table 3.

The SNR of one-stage and two-stage self-seeding at saturation are 90 and 80 respectively. The output energy of one-stage and two-stage are roughly the same (Fig 5).

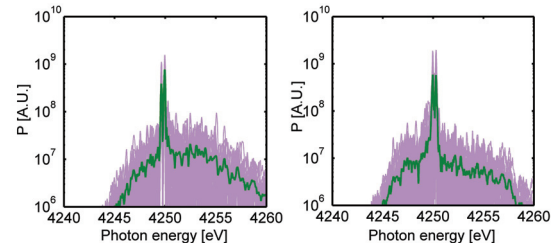


Figure 5: (Left) The saturation spectrum of 4.25 keV one-stage self-seeding. (Right) The saturation spectrum of 4.25 keV two-stage self-seeding. The green curve refers to the average. The purple curves refer to single shot.

SUMMARY

For LCLS-II HXRSS project, the instantaneous dose on the crystal is much smaller than the graphitization threshold. The average power density on the crystal of one-stage and two-stage schemes are smaller than the damage threshold measured in the experiment. The reasons why we do not choose two-stage scheme are listed in the following. (1) The heat load on the crystal is smaller than the damage threshold whether it is one-stage or two-stage self-seeding scheme. (2) For two-stage self-seeding scheme, the seed power after the first is too small to dominate the shot noise power, especially when the machine is operated in high photon energy regime. (3) The output pulse energy of two-stage is smaller than one-stage self-seeding scheme. (4) The output undulator part of one-stage scheme has two more undulator cells than that of two-stage scheme. In summary, One-stage scheme is suggested in LCLS-II HXRSS scheme, and the optimal location of the self-seeding station is slot 14.

ACKNOWLEDGEMENTS

The work was supported by the US Department of Energy (DOE) under contract DE-AC02-76SF00515 and the US DOE Office of Science Early Career Research Program grant FWP-2013-SLAC-100164.

REFERENCES

- [1] P. Emma *et al.*, “First lasing and operation of an angstrom-wavelength free-electron laser”, *Nat. Photon.*, vol. 4, pp. 641-647, 2010.

- [2] J. Amann *et al.*, “Demonstration of self-seeding in a hard-x-ray free-electron laser”, *Nat. Photon.*, vol. 6, pp.693-698, 2012.
- [3] J. Feldhaus *et al.*, “Possible application of x-ray optical elements for reducing the spectral bandwidth of an X-ray SASE FEL”, *Optics Communications*, vol. 140, pp.341-352, 1997.
- [4] G. Geloni *et al.*, “A novel self-seeding scheme for hard X-ray FELs”, *J. Mod. Opt.*, vol. 58, pp.1391-1403, 2011.
- [5] Y. Feng, “Photon Collimators – Fault Signal Generation and Detection”, LCLS-II Technical Note, 2017.
- [6] K.-J. Kim *et al.*, “An Oscillator Configuration for Full Realization of Hard X-ray Free Electron Laser”, in *Proc. IPAC'16*, Busan, Korea, May 2016, paper MOPOW039, pp. 801–804.
- [7] G. Geloni *et al.*, “Cascade self-seeding scheme with wake monochromator for narrow-bandwidth X-ray FELs”, DESY 10-080, 2010.
- [8] C. Yang *et al.*, “Distributed Self-Seeding scheme for LCLS-II”, in *Proc. FEL'17*, Santa Fe, NM, USA, Aug. 2017, paper MOP018, pp.68–70.
- [9] S. Reiche, “Genesis 1.3: a fully 3d time-dependent FEL simulation code”, *NIMA*, vol. 429, pp.243–248, 1999.
- [10] ESRF. X-ray Oriented Programs Software Package. <https://www1.aps.anl.gov/Science/Scientific-Software/XOP>